On the long-term delayed strain of concrete structures

Abudushalamu Aili, Jean-Michel Torrenti, Jean-Philippe Sellin, Jean-François Barthélémy, Matthieu Vandamme

On the long-term delayed strain of concrete structures

A. Aili[1], J.M. Torrenti[2,*], J. P. Sellin[3], J.F. Barthelemy[3], M. Vandamme[4]

1 Graduate School of Environmental Studies, Nagoya University, Japan

2 Univ Gustave Eiffel, CEREMA, UMR MCD, F-77454 Marne - la- Vallée, France

3 CEREMA, Univ Gustave Eiffel, UMR MCD, F-77171 Sourdun, France

4 Navier, École des Ponts, Univ Gustave Eiffel, CNRS, Marne-la-Vallée, France

*: Corresponding author: jean-michel.torrenti@univ-eiffel.fr

Abstract

Creep and shrinkage of concrete are essential for the safety assessment of large civil engineering structures. The present paper presents two different approaches to predicting the delayed strain considering a single material point to represent the structure. The first one is a decoupled approach, such as design codes, that splits the delayed strain into four components and predicts each of them as a function of several parameters such as concrete strength. In the second approach, delayed strain is modeled as the viscoelastic response of concrete to applied external loads and/or internal hygric stresses. The advantages and inconveniences of both methods are discussed. In the end, delayed strains of concrete are predicted using these approaches for two examples of real structures: a prestressed concrete bridge and a mock-up of a biaxially prestressed containment building.

Keywords: Concrete (E), Creep (C), Shrinkage (C), Long-term performance (C), Drying

1 Introduction

For sensitive structures such as prestressed bridges or nuclear containment, the prediction of delayed deformations is crucial. Indeed, due to these deformations, a loss of prestressing is observed with structural consequences such as large deflections of bridges [1,2], implying repairs and retrofits, which increase the likelihood of accidental damage, as was the case with the rupture of the Palau Bridge [3,4]. In the case of nuclear power plants, the prediction of the delayed deformation is crucial in view of an extension of the service life [5,6].

In the last decade or two, a variety of works have attempted to predict the macroscopic creep or shrinkage behavior of cement-based materials from the smallest scale by using micromechanics. A recent benchmark [7] compares for instance the performance of homogenization schemes for nonaging basic creep of cementitious materials derived by three different groups in the framework of continuum mechanics. Such homogenization models are also available for ageing creep (see for instance [8, 9, 10]), to make it possible to predict the creep behavior of cementitious materials from the early age. Homogenization can also be performed numerically, for instance with the Fast Fourier Transform [11]. Not only can micromechanics be used to predict macroscopic behavior, it can also be used to identify creep properties at the lower scale from macroscopic measurements (see, e.g., [7] or [11]). For what concerns shrinkage, in the same spirit, Aili et al. [12] showed that the macroscopic material properties that govern autogenous shrinkage can be obtained by homogenization. Other example, Agofack et al. [13] predict early-age macroscopic shrinkage of cement with a chemo-poro-elastoplastic model employing homogenization. The goal of micromechanical modeling is to make it possible to predict macroscopic mechanical behavior from the microstructure and microscopic mechanical properties, where the microstructure can be obtained for instance from hydration models.

Once the microscopic mechanical properties known, homogenization schemes coupled with hydration models should make it possible to predict macroscopic mechanical properties for a variety of mix designs, without needing to be calibrated with further experiments for each mix design.

There are still discussions about the physical aspects concerning creep and shrinkage. Nevertheless, it is conventionally admitted in modern codes, at a macroscopic level, that in the absence of drying, delayed deformation is decomposed into a part of (autogenous) shrinkage (in the absence of mechanical load) and a part of (basic) creep (which is the additional delayed deformation due to the presence of mechanical load). Of course, these macroscopic effects are due to phenomena occurring at smaller scales. Autogenous shrinkage is related to cement hydration, which induces self-desiccation. Consequently, capillary forces due to the decrease in internal relative humidity could explain the shrinkage [12, 14]. Note that other hypotheses, such as the existence of colloidal eigenstresses, are possible [15] and that, maybe, a coexistence of the phenomena exists: the effect of eigenstresses is particularly significant at early age when the effect of hydration evolves significantly over time. Concerning basic creep, the main assumption is that basic creep is due to shear slip at overstressed creep sites [16,17]. It has also been proposed that basic creep originates from microprestress relaxation [16], local microscopic relaxations [18], or dissolution-precipitation phenomenon [19, 20, 21]. There is still a discussion about these phenomena and their importance because it is very difficult to quantify their effect. But C-S-H plays a major role in the phenomenon because a back-analysis of creep tests with different water-to-cement ratios and different supplementary materials shows an intrinsic viscous behavior, in the sense that the viscous behavior of C-S-H does not depend on mix desing [22].

When drying occurs, additional delayed strains are observed, including drying shrinkage and drying creep. As drying is a diffusive process, the size of the structural elements and the relative humidity influence the magnitude and kinetics of drying shrinkage and drying creep. On a smaller scale, capillary forces could also explain the drying shrinkage. For drying creep, two main phenomena should be considered. The first one is the structural effect since drying is non-uniform and induces cracking at the surface of the concrete elements in the case of load-free tests [23]. When loading is applied (for instance, during a creep test or when prestressing is used), thanks to the load, less cracking and hence a larger delayed deformation due to shrinkage would be measured [24,25]. But the structural effect could not explain the drying creep amplitude alone, indicating a part of the drying creep is intrinsic to the material [26]. The origin of this intrinsic part of the drying creep is still discussed. Several explanations are possible such as the microdiffusion of water [27], the lubricant role of water diffusion [28, 29], or the coupling between capillary forces and an external loading [30]. Finally, a hygro-mechanical coupling has been highlighted which can explain a small part of the deformations [31]. Examples of modeling studies based on the multi-scale and multi-physics approach and its application of the method to real bridges are presented in Maekawa's pioneering work [32,33] and other examples [34, 35].

In the following, only a macroscopic approach will be used to show its application to real structures. The macroscopic models reflect as much as possible the influence of major phenomena of the lower scale: drying, the strength of concrete (reflecting the role of the water-to-cement ratio), and the type of cement (or the use of supplementary cementitious materials). But, of course, information is lost when going from the micro to the macro scale with as consequence a possible discrepancy between measurements on structures and modeling. This can be compensated by adjusting the parameters of the shrinkage and creep laws based on the deformations of the structure considered or on laboratory specimens when they are available. After a presentation of two models that will be used, an application

of this strategy to the case of a real bridge and a one-third mockup of a nuclear power plant vessel will be described.

2 Modeling

Two macroscopic approaches are possible for the modeling of delayed behavior. The first is conventional methods used in most design codes like EC2 [36] or fib models like actual MC2010 [37] or the future MC2020. This approach splits the delayed deformations into four uncoupled components: autogenous shrinkage, drying shrinkage, basic creep, and drying creep. The other is a fully coupled approach without assuming the classical decomposition of delayed strain above. Note that the two approaches are used here at the level of a single material point, using analytical relations. Consequently, taking into account phenomena like the structural part of the drying creep could not be considered because taking it into account would require finite element modeling to consider humidity and stress gradients.

2.1 Modeling with four components using codes for design

An example of the approach with four components of delayed strain is MC2010 [37]. Note that this approach is very similar to the one of the future EC2 [38], which adds the possibility to adjust the parameters of the equations governing the different components to experimental results. Shrinkage and creep are predicted as a function of the strength of concrete, the type of cement, the relative humidity of the environment, the notional size of the structure, and the loading age. This model is relatively simple because it should be applied by engineers for cross-section calculations at a stage where concrete is only defined by its strength. Of course, a lot of parameters are not considered. For example, aggregate content, type, and Young's modulus are very influential on concrete creep and shrinkage but are not considered by the codes. It is the same for the quality of the binder (water-to-cement ratio, quantity of binder, use of SCMs…) which is not considered while all the micro-scale studies have shown its importance on delayed strains. Decoupling is also a simplification that will be discussed later.

The model reads as follows. The delayed strain ε^c of concrete is the sum of basic shrinkage ε^{bs} (i.e., autogenous shrinkage), drying shrinkage ε^{ds}, basic creep ε^{bc}, and drying creep ε^{dc}.

$$\varepsilon^c = \varepsilon^{bs} + \varepsilon^{ds} + \varepsilon^{bc} + \varepsilon^{dc}. \quad (1)$$

Basic shrinkage ε^{bs} and drying shrinkage ε^{ds} are expressed as:

$$\varepsilon^{bs} = \xi_{cbs1}\alpha_{bs}\left(\frac{0{,}1\, f_{cm}}{6+0{,}1\, f_{cm}}\right)\left(1 - e^{-0{,}2\xi_{cbs2}\sqrt{t}}\right), \quad (2)$$

$$\varepsilon^{ds} = \xi_{cds1}\left[(220 + 110\alpha_{ds1})e^{-\alpha_{ds2} f_{cm}}\right]\beta_{RH}\left[\frac{(t-t_s)}{0{,}035\xi_{cds2}h^2+(t-t_s)}\right]^{0,5}, \quad (3)$$

with α_{bs}, α_{ds1} and α_{ds2} are parameters that depend on the type of cement, h is the notional size of the considered structure (equal to $A_c/2p$, where A_c is the cross-section and p is the perimeter) in millimeters; $f_{cm}$is the strength of concrete in MPa; t_s is the age of the concrete in days at the start of drying; ξ_{cbs1} , ξ_{cds1}, ξ_{cbs2} and ξ_{cds2} are the parameters introduced to give the possibility to adjust the predictions to experimental results (the default values are equal to 1). β_{RH} is a function of the relative humidity RH, given in MC2010.

Basic creep $\varepsilon^{bc}$and drying creep ε^{dc} are expressed respectively by basic creep function $\varphi_{bc}(t,t_0)$ and drying creep function $\varphi_{dc}(t,t_0)$, i.e., $\varepsilon^{bc}(t,t_0) = \frac{\sigma_0}{E_c}\varphi_{bc}(t,t_0)$ and $\varepsilon^{dc}(t,t_0) = \frac{\sigma_0}{E_c}\varphi_{dc}(t,t_0)$, where

σ_0 is the applied constant stress, E_c is the tangent modulus of elasticity and t_0 is the age of the concrete at loading. Basic creep function and drying creep function read:

$$\varphi_{bc}(t,t_0) = \xi_{bc1}\frac{1.8}{(f_{cm})^{0.7}} ln\left(1 + (\frac{30}{t_{0,adj}} + 0.035)^2 \frac{(t-t_0)}{\xi_{bc2}}\right), \quad (4)$$

$$\varphi_{dc}(t,t_0) = \xi_{dc1}\beta_{dc}(f_{cm}, RH, t_0, \xi_{dc2})\, \beta_{dc,t-t0} \quad (5)$$

with $t_{0,adj}$ is the adjusted age at loading of the concrete based on the type of cement and the curing temperature; ξ_{bc1}, ξ_{bc2}, ξ_{dc1} and ξ_{dc2} are parameters that may be adjusted according to the experimental results. The expressions of β_{dc} and $\beta_{dc,t-t_0}$ are:

$$\beta_{dc}(f_{cm}, RH, t_0) = \frac{412}{(f_{cm})^{1.4}} \frac{1 - \frac{RH}{100}}{\sqrt[3]{0.1\frac{h}{100}}} \frac{1}{0.1 + (t_{0,adj})^{0.2}} \quad (6)$$

$$\beta_{dc,t-t0} = \left[\frac{t - t_0}{\xi_{dc2}\beta_h + t - t_0}\right]^{\gamma(t_0)} \quad (7)$$

$$\gamma(t_0) = \frac{1}{2.3 + 3.5/\sqrt{t_{0,adj}}} \quad (8)$$

$$\beta_h = \min\{1.5h + 250\left(\frac{35}{f_{cm}}\right)^{0.5}, 1500\left(\frac{35}{f_{cm}}\right)^{0.5}\} \quad (9)$$

where h is the notional size. Table 1 summarizes the used parameters.

Table1: Parameters of equations 4 to 9

t_0	Age at loading
$t_{0,adj}$	Adjusted age at loading of the concrete based on the type of cement and the curing temperature
RH	Ambient relative humidity
H	Notional size = half cross-section divided by the perimeter of the section
ξ_{bc1}, ξ_{bc2}, ξ_{dc1} and ξ_{dc2}	Parameters that could be adjusted to experimental results; default values = 1
f_{cm}	Mean compressive strength

These functions are empirical but take into account the influence of the strength, RH, age at loading and size of the concrete structures which are the main physical parameters influencing the drying creep.

The predicted strains are not local strains but are related to the cross-section of the considered concrete member. It means that internal stresses are not predicted using this approach. The advantage of this approach is the simplicity for the use of engineers, but one drawback is the fact that the phenomena are uncoupled. In a real structure, concrete is affected by drying. But basic creep decreases when the internal relative humidity decreases. This has been demonstrated on a macroscopic scale with basic creep tests on samples that were submitted to drying before the creep test [39, 40] and, recently, using micro-indentation [41–44]. The consequence is that for a loaded drying specimen, because drying creep is obtained by subtracting the basic creep from the total creep, estimation of its basic creep from a companion non-drying specimen would result in an underestimated drying creep. Moreover, the two parts' kinetics are different - basic creep is

logarithmic while drying creep is asymptotic [45, 46]. The size of the concrete members affects drying creep but not basic creep. As a result, the decoupled modeling of basic creep and drying creep impacts the prediction of the long-term behavior of concrete structures. Hence, the need for a fully coupled approach has arisen.

2.2 Modeling with a fully coupled approach

One of the examples of a fully coupled approach was developed by Aili et al. [47]. They regarded concrete as viscoelastic porous material subjected to externally applied loads and internal hygric stress (i.e., capillary pressure) due to drying or self-desiccation. The compliance of concrete was considered dependent on the internal relative humidity. The delayed behavior of concrete was then modeled as linear viscoelastic strain. In this model, the four components of decoupled method correspond approximately to the following: autogenous shrinkage and drying shrinkage as the viscous response of concrete to the capillary pressure, respectively, due to self-desiccation and drying; basic creep as a viscous response to the applied load; drying creep as the viscous response to an amplified part of the capillary pressure in the presence of compression load (as proposed by Sellier et al. [31]).

This model has some simplifications when the micro-scale is considered: firstly, it is a non-aging model meaning that hydration is not considered and early age could not be addressed. Then, to consider only capillary forces, its applicability is limited to relative humidities between 100% and 40%. Note also that for drying creep, as explained later, a fitting of experimental results is needed.

In the following, the model is briefly presented. Stress-strain relationships are given in terms of volumetric and deviatoric components. For the volumetric part, the mean stress $\sigma_v = tr(\underline{\sigma})/3$ (where $\underline{\sigma}$ is stress tensor) is related to volumetric strain $\varepsilon_v = tr(\underline{\varepsilon})$ (where $\underline{\varepsilon}$ is strain tensor) via:

$$\varepsilon_v^e + \varepsilon_v^c = \int_{-\infty}^{t} J^K(t-\tau)\frac{d\sigma_v'(\tau)}{d\tau}d\tau, \tag{10}$$

where J^K is the bulk creep compliance, ε_v^e is the elastic strain, and σ_v' is effective mean stress. To compute the strain evolution $\varepsilon_v^c(t)$ over time, we need to assess the creep compliance J^K and effective stress evolution σ_v', both of which depend on the drying state (more specifically, the internal relative humidity $h_r(t)$ and saturation degree $S_L(t)$).

On the one hand, the bulk creep compliance reads as:

$$J^K(T, h_r, t-t_0) = \frac{1}{K} + \frac{1}{C(h_r)} ln\left(1 + \frac{t-t_0}{\tau(T)}\right), \tag{11}$$

where K is the elastic bulk modulus, C and τ are the creep compliance and characteristic time, depending respectively on the relative humidity and temperature.

On the other hand, the effective volumetric stress σ_v' is assessed in time-incremental form by:

$$d\sigma_v' = d\sigma_v - \kappa d\sigma_h, \tag{12}$$

where κ and σ_h are respectively the drying creep coefficient and pore water stress. Drying creep coefficient κ equals 1 in the case of drying with no load, whereas it is larger than 1 for cases of drying under compression load. Its value needs to be fitted with experimental results. Pore water stress σ_h can be computed from capillary pressure $P_c(S_L)$ by:

$$\sigma_h(t) = \int_{-\infty}^{t} b(t-\tau)\frac{d\big(S_L(\tau)P_c(\tau)\big)}{d\tau}d\tau, \tag{13}$$

where b is the viscoelastic Biot coefficient. For the details related to the computation of the parameters P_c, b, the function of $C(h_r)$, and the deviatoric stress-strain relationship, readers are invited to see the original model in [47].

The model is based on the physical origin of the delayed strain, and the coupling between different components of delayed strain is considered. As mentioned in the introduction, several hypotheses exist in the literature to explain the origin of drying creep. The present model provides an alternative way (see section 9.1 of [47]) to follow the explanation of the lubricant role of water diffusion. The delayed strain of various drying/loading cases is modeled in a unified manner, with only one fitting parameter, drying creep coefficient κ. The influence of varying temperature and relative humidity can be integrated easily. Since the model is written in integral form like design codes (e.g., MC2010), it can be easily applied in engineering practice. However, it should be kept in mind that a constant drying creep coefficient assumption is a strong simplification. Instead, the creep coefficient should be related to the intensity of drying and the mechanical load. Another drawback of the model is that its implementation in conventional finite element codes in the framework of the superposition principle is not direct since various parameters (stress, temperature, and RH histories) in all previous steps are needed to calculate the next step. It is, of course, possible to store these parameters at each time step for each Gaussian point but it means working with large tables in the calculations.

3 Application to real structures

The best way to apply these approaches to predict the very long-term behavior of real structures appears to be fitting the parameters of the constitutive relations. This was for instance proposed for the prediction of the deflections of long-span prestressed bridges [48]. Indeed, the parameters of the codes are mainly dependent on the compressive strength. It is possible to obtain the same strength with different concrete mixes, especially where low-carbon concretes are developed. As a result, the variability of the creep is very high. For instance, in the future Eurocode 2 [49], the 5% fractile of the distribution of the creep coefficients $\varphi(t, t_0)$ corresponds to $0{,}5\ \varphi(t, t_0)$ and the 95% fractile to $1{,}4\ \varphi(t, t_0)$.

Estimation of long-term delayed strain is presented with two examples: a prestressed concrete bridge and a mock-up of a biaxially prestressed concrete containment building.

3.1 Application to the Savines bridge

The Savines Bridge (France) is a post-tensioned prestressed concrete bridge constructed between 1958 and 1960 by the free cantilever method. It is a 77 m long box-girder bridge made of 13 spans, each of them consisting of 22 cast-in-place segments with depths varying from 4.15 m at main piers to 1.15 m at mid-span (see Figure 1). Each span consists of two cantilevers connected by hinge devices located at the mid-span sections. These hinge devices are materialized by a steel ball-and-socket arrangement allowing free horizontal displacement and rotation at mid-span. In Figure 1, this configuration leads to large deflections that are visible. Figure 2 presents the evolution of the deflection at the mid-span of the section between piers P6 and P7. It can be seen that the deflection evolves as a logarithmic function of time.

Figure 1 View of the Savines bridge. The hinges allow large deflections that are visible at each mid-span (photo credited to J.M. Torrenti)

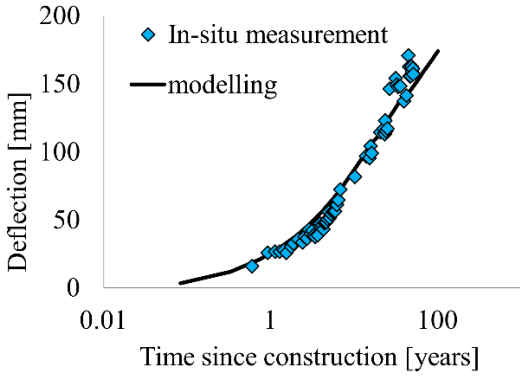

Figure 2 Evolution of the measured deflection at mid-span of the section between piers P6 and P7, data from [50] and comparison with the adjusted model. Note that the measurement baseline has changed over time and the evolution of the deflection was adjusted to obtain continuity (but with an important uncertainty). It implies it is difficult to comment on the difference existing at later ages.

A previous study [50] has shown that it is possible to adjust the parameters of the relations proposed in codes for the amplitude and kinetics of basic and drying creeps, autogenous and drying shrinkages. The predicted amplitudes of the strains were multiplied by a weighting factor to adjust the measured deflections (and the kinetics were unchanged). The best prediction of deflections (Figure 2), obtained from the least square method, gave the optimum values of the weights. The amplitudes of drying shrinkage, basic creep, and drying creep were multiplied by 1.6, 1.6, and 1.4, while autogenous shrinkage remained unchanged. These values are slightly higher than the 95% fractile indicated in the future EC2 but could be explained by the fact that this bridge is particularly sensitive to delayed strains due to its specificity (hinges in the middle of each span). It should be pointed out that the optimization of the parameters does not give a unique solution: it is possible with several choices to adjust the model to fit the experimental deflection. For instance, part of the delayed deflection could also be explained by the loss of prestressing in cantilever tendons [51].

This study considered the effect of shear forces at mid-span [2]. Indeed, in bridges built by the cantilever method, these forces could play an important role, and their effect on delayed deflections

is not negligible. This study emphasizes that the modeling practice must consider precisely the delayed strains in the material and deserves a keen understanding of the concrete structure behavior with its environment.

3.2 Application to the VeRCoRs mock-up

VeRCoRs is a mock-up at the 1/3 scale of a biaxially prestressed concrete containment of a nuclear power plant [52]. It is highly instrumented to monitor its behavior. The in-situ measurement recorded the temperature, relative humidity, and strain of the structure. In addition, using concrete from the same casting as the mock-up, cylindrical samples of 1 m height and 22 cm diameter were prepared. Tests were performed on these samples in laboratory conditions (temperature equal to 20°C, and the relative humidity for drying samples equal to 50%) to characterize the delayed strain behavior under four different conditions:

- test 1) sealed load-free i.e. autogenous shrinkage measurement;
- test 2) drying load-free giving drying shrinkage by subtraction of autogenous shrinkage;
- test 3) sealed and loaded giving basic creep by subtraction of autogenous shrinkage;
- test 4) drying and loaded giving drying creep by subtraction of autogenous and drying shrinkages and basic creep.

In the following, we use the results of the four tests to fit the two models in section 2 and predict the delayed strain of the mock-up under the prestressing load, recorded temperature, and relative humidity. We consider a small unit of the material unit in the mock-up, subjected to a vertical stress of 6.3 MPa and a horizontal stress of 10.6 MPa. These stresses correspond to the prestress in vertical and horizontal prestressing tendons and are to relax over time. The vertical prestress was applied 15 days later than the horizontal one. Based on the recorded temperature and relative humidity, we consider the simplified temperature and relative humidity history shown in Figure 3. The complete history of the temperature and RH measurements was recently published in a paper concerning the Vercors mockup [39]. The real variations of the relative humidity are more complicated than our simple assumption and it could certainly be an improvement to consider the real history in a future calculation.

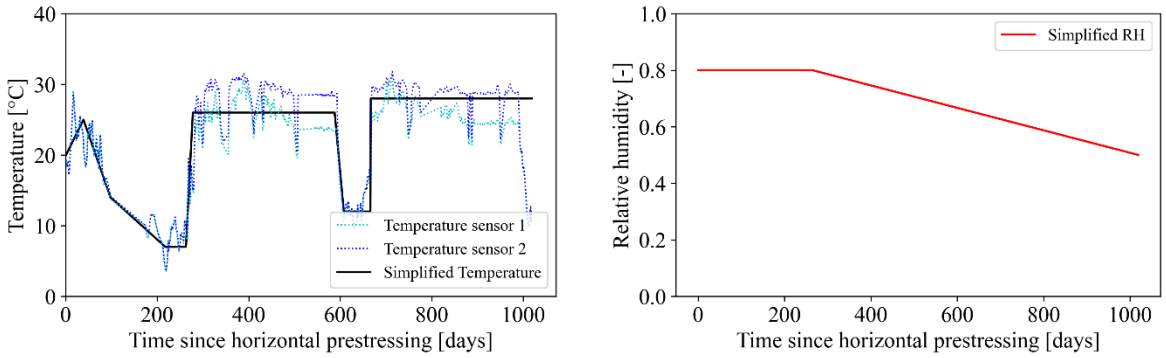

(a) (b)

Figure 3 Simplified temperature (a) and RH (b) history for the modeling of the mock-up. Recorded temperature by two sensors are also shown in (a).

For the decoupled modeling with MC2010 in section 2.1, the measured time evolutions of the creep and shrinkage tests 1-4 were calibrated to Eqs. 2-9 by adjusting the fitting parameters. The best-fit parameters are listed in 2. Except for basic shrinkage where equation 1 was not adapted to the experimental results (but basic shrinkage is not very important in this application because prestressing was applied when the concrete was older than 3 months), the parameters corresponding to the amplitude of the phenomena (subscript 1) are close to 1 for drying shrinkage but larger for basic and drying creeps. A comparison of the results of the use of this model with the fitted parameters and the default values (1 for all the parameters of table 2) is presented in figure 4. The difference highlights the importance of this fitting procedure to obtain a good prediction of the delayed strains because code relations only give mean values. Then, inserting these values together with the thickness, temperature, and relative humidity of the mock-up into Eqs.2-9, we can estimate the time evolution of the delayed strain of the mock-up. The prediction can also be performed considering the stress relaxation in reinforced tendons. Details of the coupling between the relaxation of tendons and delayed strain of concrete were previously described in [53] and omitted here since it is out of the main scope of the article.

Table 2 Fitting parameters for the four components of delayed strain in Eqs.2-9 in MC2010

Basic shrinkage		Drying shrinkage		Basic creep		Drying creep	
ξ_{cbs1}	ξ_{cbs2}	ξ_{cds1}	ξ_{cds2}	ξ_{bc1}	ξ_{bc2}	ξ_{dc1}	ξ_{dc2}
152	0.002	0.8	0.4	2.1	1.6	1.6	3.4

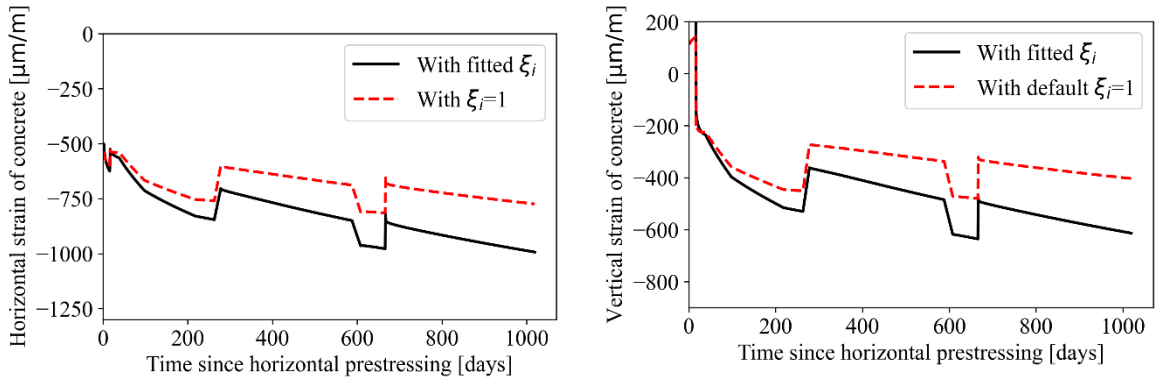

(a) (b)

Figure 4: comparison of the predicted horizontal (a) and vertical (b) strains of the Vercors mockup in the case of default values ($\xi_i = 1$) or fitted values for the coefficients ξ_{cbs1}, ξ_{cds1}, ξ_{cbs2}, ξ_{cds2}, ξ_{bc1}, ξ_{bc2}, ξ_{dc1} and ξ_{dc2}

For the coupled approach with the model in section 2.2, firstly, we compute the basic creep as the difference of measured strain in tests 3 and test 1. Then, considering the viscoelastic Poisson's ratio as 0.2 based on the collected database in [54], the creep compliance in Eq.11 is fitted against the basic creep to obtain the bulk elastic modulus $K = 17$ GPa, creep modulus $C_{sat} = 70$ GPa and characteristic time $\tau_0 = 44$ d under constant relative humidity and constant temperature.

Secondly, the creep compliance is assessed by considering its dependency on temperature and relative humidity. For the variation of the creep modulus C in function of relative humidity, we based ourselves on the microindentation test of [43]. Given the water-to-cement ratio of the concrete used in the

mock-up is 0.52, we considered only the indentation creep modulus of the cement pastes with water-to-cement ratio of 0.55 from [43], as shown in Figure 4. During the decrease of relative humidity, the ratio between the increase $C(h_r) - C_{sat}$ of creep modulus to the creep modulus C_{sat} at the saturated state can be regarded to be a linear function of the relative humidity:

$$\frac{C(h_r) - C_{sat}}{C_{sat}} = 5(1 - h_r). \tag{14}$$

Then, we assume that, for the mock-up, the creep modulus varies following Eq.14 as a function of relative humidity over time. For the characteristic time of creep, referring to [55], thermo-activation is applied as follows:

$$\tau(T) = \tau_0 \exp\left(Q\left(\frac{1}{T} - \frac{1}{T_0}\right)\right), \tag{15}$$

where Q=2500 K is the activation energy of water viscosity [56], T and T_0=293.15 K are the current temperature and temperature of the reference test in Kelvin.

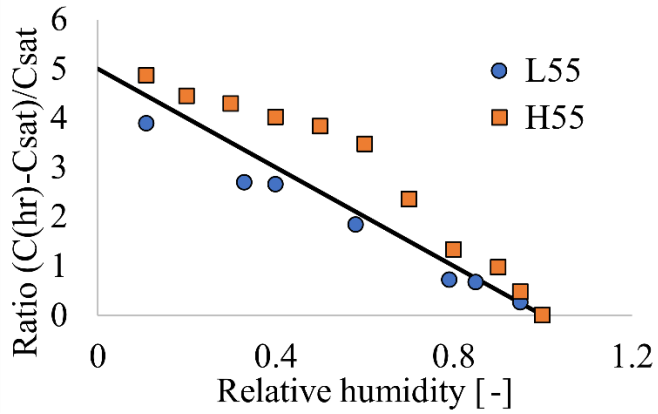

Figure 54 Variation of creep modulus of cement pastes in function of relative humidity, data from [43]. L55 and H55 are low-heat and high early-strength Portland cement pastes, respectively. Their water-to-cement ratio is 0.55.

Thirdly, the evolutions of relative humidity and pore water pressure are assessed based on the desorption isotherm measured on the samples under the same drying conditions as tests 2 and 4 [57]. The desorption isotherm (Table 3) gives the relationship between saturation degree S_L and relative humidity h_r. Capillary pressure P_c is calculated from Kelvin's law [12]. Knowing the evolution of S_L and P_c in test 2 and test 4, on the one hand, we can check the quality of the fitting by comparing the strain of test 2 with the predicted strain by Eqs.10-13 using $\kappa = 1$. On the other hand, by fitting the strain predicted by Eqs.10-13 against the strain results of test 4, we obtain the creep coefficient $\kappa = 1.7$ for the case of drying with the presence of load. Table 4 summarizes the fitted parameters of the coupled model.

Table 3. Desorption isotherm

HR (%)	*100*	97	92	84	75	58	43	23	*0*
S (%)	*100*	86.7	79.4	67.5	53.6	37.2	25.5	15.2	*0*

Table 4. Fitted parameters of the coupled model.

Young's modulus [GPa]	Uniaxial creep modulus [GPa]	Creep characteristic time [days]	Poisson ratio [-]	Elastic Biot coefficient [-]	Long-term Biot coefficient [-]	Drying creep coefficient κ [-]	Sorption isotherm a_1 [-]	Sorption isotherm b_1 [MPa]
30	126	44	0.2	0.33	0.79	1.7	0.44	19

Finally, we predict the strain evolution of the considered unit of material in the mock-up, under the vertical and horizontal stress and temperature and relative humidity history shown in Figure 3.

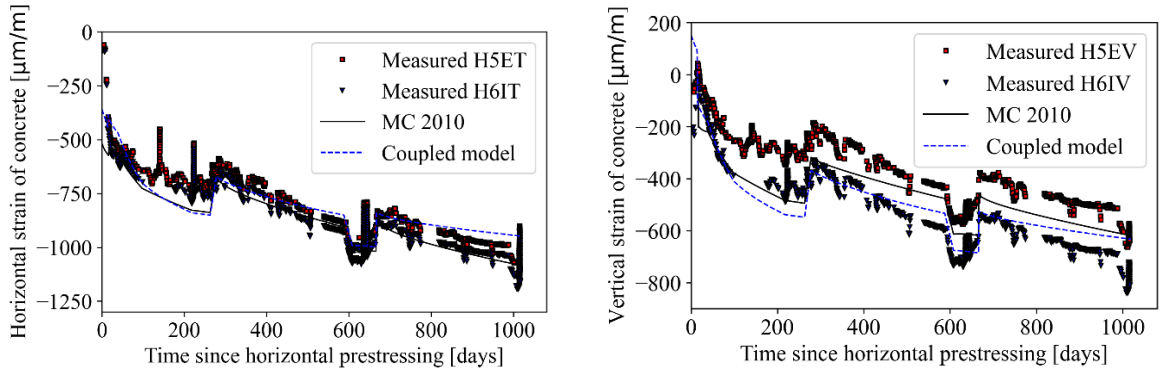

(a) (b)

Figure 6 Comparison of measured and predicted strain of the VeRCoRs mock-up: (a) horizontal strain; (b) vertical strain.

The predictions of the MC2010 and coupled model are compared with in-situ measured data in Figure 6. Measured data are from two sensors, H5E and H6I, located at mid-height of the mock-up, far from unusual features like the hatch. H5E was placed 7.6 cm away from the external surface of the mock-up and H6I 7.3 cm away from the internal surface. It can be seen that, despite simulation of a single material point, the prediction of long-term delayed strains by the two modelings are within the range of variations of measured strain by the two sensors. Compared with the rate of increase of the delayed strains of measurement in the long term, the predictions of the MC2010 model seem better than that of the coupled model. The lower quality of the prediction of the latter one may be because the structural part of drying creep is not considered here. Another limitation of the coupled model is the isotropic choice of parameter κ. It should also be noted that these results certainly depend on the size of the considered structure and could not be generalized.

4. Conclusions

We presented two different methods to predict the delayed strains of concrete. The first is similar to the methods of design codes, such as the fib model codes MC2010 and MC2020. This method splits the delayed strain into four components: autogenous shrinkage, drying shrinkage, basic creep, and drying creep, and considers them independent from each other. The other is a fully coupled approach that models the four components in a unified manner. This method is based on the physical origin of the delayed strains and considers potential coupling between different components.

The first model is applied to a bridge and the two models are applied to the mock-up of a nuclear containment vessel. The results show that, by fitting the parameters of the models to experimental

results of laboratory testing, the evolution of long-term deformation of the real structures can be relatively well estimated. We infer that the fitting parameters of both approaches can reproduce the involved physical phenomena.

With the promotion of low-carbon construction, concretes with the same strength will have very different mix-design. The delayed strains of these concrete structures can differ from each other significantly. In these cases, we need models providing the possibility to fit parameters with laboratory experiments, such as the above two models.

Acknowledgments

The first, second, and fifth authors acknowledge financial support from EDF for the part of the research concerning the development of the coupled model.

References

[1] Z.P. Bazant, M.H. Hubler, Q. Yu, Excessive Creep Deflection: An Awakening, Concr. Int. 33 (2011) 44–46.

[2] J.P. Sellin, H. Sousa, J.F. Barthélémy, J.M. Torrenti, Novel semi-analytical model to calculate shear forces due to viscoelastic interactions, Eng. Struct. 183 (2019) 999–1013. https://doi.org/10.1016/j.engstruct.2018.12.015.

[3] Z.P. Bažant, Q. Yu, G.-H. Li, Excessive Long-Time Deflections of Prestressed Box Girders. I: Record-Span Bridge in Palau and Other Paradigms, J. Struct. Eng. 138 (2012) 676–686. https://doi.org/10.1061/(asce)st.1943-541x.0000487.

[4] C. Burgoyne, R. Scantlebury, Why did Palau Bridge collapse?, Struct. Eng. 84 (2006) 30–37.

[5] F. Benboudjema, J.M. Torrenti, On the Very Long-Term Delayed Behavior of Biaxially Prestressed Structures: The Case of the Containments of Nuclear Power Plants, in: CONCREEP 10, 2015: pp. 631–639.

[6] H.W. Song, S.H. Kim, K.J. Byun, Y.C. Song, Creep prediction of concrete for reactor containment structures, Nucl. Eng. Des. 217 (2002) 225–236. https://doi.org/10.1016/S0029-5493(02)00135-8.

[7] Königsberger, Markus, Túlio Honório, Julien Sanahuja, Brice Delsaute, et Bernhard LA Pichler. « Homogenization of nonaging basic creep of cementitious materials: A multiscale modeling benchmark ». Construction and Building Materials 290 (2021): 123144

[8] Honorio, Tulio, Benoit Bary, et Farid Benboudjema. « Multiscale estimation of ageing viscoelastic properties of cement-based materials: A combined analytical and numerical approach to estimate the behaviour at early age ». Cement and Concrete Research 85 (2016): 137-55.

[9] Scheiner, S., et C. Hellmich. « Continuum Microviscoelasticity Model for Aging Basic Creep of Early-Age Concrete ». Journal of Engineering Mechanics 135, n° 4 (avril 2009): 307-23. https://doi.org/10.1061/(ASCE)0733-9399(2009)135:4(307).

[10] Sanahuja, Julien, et Shun Huang. « Mean-field homogenization of time-evolving microstructures with viscoelastic phases: application to a simplified micromechanical model of hydrating cement paste ». Journal of Nanomechanics and Micromechanics 7, n° 1 (2017): 04016011.

[11] Šmilauer, Vít, et Zdeněk P. Bažant. « Identification of viscoelastic C-S-H behavior in mature cement paste by FFT-based homogenization method ». Cement and Concrete Research 40, n° 2 (février 2010): 197-207. https://doi.org/10.1016/j.cemconres.2009.10.003

[12] Aili, Abudushalamu, Matthieu Vandamme, Jean-Michel Torrenti, et Benoit Masson. « Is long-term autogenous shrinkage a creep phenomenon induced by capillary effects due to self-desiccation? » Cement and Concrete Research 108 (juin 2018): 186-200. https://doi.org/10.1016/j.cemconres.2018.02.023

[13] Agofack, Nicolaine, Siavash Ghabezloo, et Jean Sulem. « Chemo-Poro-Elastoplastic Modelling of an Oilwell Cement Paste: Macroscopic Shrinkage and Stress-Strain Behaviour ». Cement and Concrete Research 132 (juin 2020): 106046. https://doi.org/10.1016/j.cemconres.2020.106046

[14] C. Hua, P. Acker, A. Ehrlacher, Analyses and models of the autogenous shrinkage of hardening cement paste. I. Modelling at macroscopic scale, Cem. Concr. Res. 25 (1995) 1457–1468. https://doi.org/10.1016/0008-8846(95)00140-8.

[15] M. Abuhaikal, K. Ioannidou, T. Petersen, R.J.M. Pellenq, F.J. Ulm, Le Châtelier's conjecture: Measurement of colloidal eigenstresses in chemically reactive materials, J. Mech. Phys. Solids. 112 (2018) 334–344. https://doi.org/10.1016/j.jmps.2017.12.012.

[16] Z.P. Bažant, A.B. Hauggaard, S. Baweja, F. Ulm, Microprestress-Solidification Theory for Concrete Creep. I: Aging and Drying Effects, J. Eng. Mech. 123 (1997) 1188–1194. https://doi.org/10.1061/(ASCE)0733-9399(1997)123:11(1188).

[17] S. Rahimi-Aghdam, Z.P. Bažant, G. Cusatis, Extended microprestress-solidification theory for long-term creep with diffusion size effect in concrete at variable environment, J. Eng. Mech. 145 (2019) 04018131. https://doi.org/10.1061/(ASCE)EM.1943-7889.0001559.

[18] M. Vandamme, Two models based on local microscopic relaxations to explain long-term basic creep of concrete, Proc. R. Soc. A Math. Phys. Eng. Sci. 474 (2018). https://doi.org/10.1098/rspa.2018.0477.

[19] I. Pignatelli, A. Kumar, R. Alizadeh, Y. Le Pape, M. Bauchy, G. Sant, A dissolution-precipitation mechanism is at the origin of concrete creep in moist environments, J. Chem. Phys. 145 (2016). https://doi.org/10.1063/1.4955429.

[20] X. Li, Z.C. Grasley, E.J. Garboczi, J.W. Bullard, Modeling the apparent and intrinsic viscoelastic relaxation of hydrating cement paste. Cement and Concrete Composites (2015) 55(Supplement C): 322-330

[21] X. Li, Z.C. Grasley, J.W. Bullard, P. Feng, Creep and relaxation of cement paste caused by stress-induced dissolution of hydrated solid components. Journal of the American Ceramic Society (2018) 101(9): 4237-4255

[22] Hu, Z., Hilaire, A., Ston, J., Wyrzykowski, M., Lura, P., & Scrivener, K. (2019). Intrinsic viscoelasticity of CSH assessed from basic creep of cement pastes. Cement and Concrete Research, 121, 11-20.

[23] Grasley, Z. C., Lange, D. A., & D'Ambrosia, M. D. (2006). Internal relative humidity and drying stress gradients in concrete. Materials and Structures, 39(9), 901-909.

[24] Z.P. Bažant, Y. Xu, Drying creep of concrete: constitutive model and new experiments separating its mechanisms, Mater. Struct. 27 (1994) 3–14. https://doi.org/10.1007/BF02472815.

[25] L. Granger, J.-M. Torrenti, P. Acker, Thoughts about drying shrinkage: experimental results and quantification of structural drying creep, Mater. Struct. 30 (1997) 588–598.

[26] Bažant, Z. P., & Yunping, X. I. (1994). Drying creep of concrete: constitutive model and new experiments separating its mechanisms. Materials and structures, 27(1), 3-14.

[27] Z.P. Bazant, J. C. Chern, Concrete creep at variable humidity: constitutive law and mechanism, Mater. Struct. 18 (1985) 1–20.

[28] I. Vlahinić, J.J. Thomas, H.M. Jennings, J.E. Andrade, Transient creep effects and the lubricating power of water in materials ranging from paper to concrete and Kevlar, J. Mech. Phys. Solids. 60 (2012) 1350–1362. https://doi.org/10.1016/j.jmps.2012.03.003.

[29] R. Sinko, M. Vandamme, Z.P. Bažant, S. Keten, Transient effects of drying creep in nanoporous solids: understanding the effects of nanoscale energy barriers, Proc. R. Soc. A Math. Phys. Eng. Sci. 472 (2016) 20160490. https://doi.org/10.1098/rspa.2016.0490.

[30] Wyrzykowski, M., & Lura, P. (2014). The effect of external load on internal relative humidity in concrete. Cement and concrete research, 65, 58-63.

[31] A. Sellier, S. Multon, L. Buffo-Lacarrière, T. Vidal, X. Bourbon, G. Camps, Concrete creep modelling for structural applications: non-linearity, multi-axiality, hydration, temperature and drying effects, Cem. Concr. Res. 79 (2016) 301–315.

[32] S. Asamoto, T. Ishida, K. Maekawa, Time-dependent constitutive model of solidifying concrete based on thermodynamic state of moisture in fine pores, J. Adv. Concr. Technol. 4 (2006) 301–323. https://doi.org/10.3151/jact.4.301.

[33] K. Maekawa, N. Chijiwa, T. Ishida, Long-term deformational simulation of PC bridges based on the thermo-hygro model of micro-pores in cementitious composites, Cem. Concr. Res. 41 (2011) 1310–1319. https://doi.org/10.1016/j.cemconres.2011.03.021.

[34] V. Kolínský, J.L. Vítek, Verification of numerical creep and shrinkage models in an arch bridge analysis, Struct. Concr. 20 (2019) 2030–2041. https://doi.org/10.1002/suco.201800203.

[35] B.I.G. Barr, J.L. Vitek, M.A. Beygi, Seasonal shrinkage variation in bridge segments, Mater. Struct. Constr. 30 (1997) 106–111. https://doi.org/10.1007/bf02486311.

[36] European Standards Institution, Eurocode 2: Design of Concrete Structures: Part 1-1: General Rules and Rules for Buildings, European Standards, London, 2004.

[37] FIB, Fib Bulletin 65: Model Code 2010, Volume 1, 2012.

[38] H.S. Müller, I. Anders, R. Breiner, M. Vogel, Concrete: treatment of types and properties in fib Model Code 2010, Struct. Concr. 14 (2013) 320–334.

[39] Z.P. Bažant, A.A. Asghari, J. Schmidt, Experimental study of creep of hardened Portland cement paste at variable water content, Mater. Struct. 9 (1976) 279–290.

[40] Wittmann, F. H. (1970). The effect of moisture content on creep of hardened cement pastes. Rheologica Acta, 9(2), 282-287.

[41] Q. Zhang, Creep properties of cementitious materials : effect of water and microstructure : An approach by microindentation, Paris-Est University, 2014.

[42] J. Frech-Baronet, L. Sorelli, J.-P. Charron, New evidences on the effect of the internal relative humidity on the creep and relaxation behaviour of a cement paste by micro-indentation techniques, Cem. Concr. Res. 91 (2017) 39–51.

[43] P. Suwanmaneechot, A. Aili, I. Maruyama, Creep behavior of C-S-H under different drying relative humidities: Interpretation of microindentation tests and sorption measurements by multi-scale analysis, Cem. Concr. Res. 132 (2020) 106036. https://doi.org/10.1016/j.cemconres.2020.106036.

[44] Liu, Y., Li, Y., Jin, C., & Li, H. (2022). Multi-scale creep analysis of cement paste–Indentation prediction and time correspondence of mechanisms. Cement and Concrete Composites, 134, 104815.

[45] J.-M. Torrenti, R. Le Roy, Analysis of some basic creep tests on concrete and their implications for modeling, Struct. Concr. 19 (2018) 483–488. https://doi.org/10.1002/suco.201600197.

[46] R. Wendner, M.H. Hubler, Z.P. Bažant, The B4 Model for Multi-decade Creep and Shrinkage Prediction, in: Mech. Phys. Creep, Shrinkage, Durab. Concr., 2013: pp. 429–436. https://doi.org/10.1061/9780784413111.051.

[47] A. Aili, M. Vandamme, J.M. Torrenti, B. Masson, A viscoelastic poromechanical model for shrinkage and creep of concrete, Cem. Concr. Res. 129 (2020) 105970. https://doi.org/10.1016/j.cemconres.2019.105970.

[48] I.N. Robertson, Prediction of vertical deflections for a long-span prestressed concrete bridge structure, Eng. Struct. 27 (2005) 1820–1827. https://doi.org/10.1016/j.engstruct.2005.05.013.

[49] European Standards Institution, Eurocode 2: Design of concrete structures—Part 1-1: General rules,rules for buildings, bridges and civil engineering structures, Brussels CEN. (2022).

[50] J.-P. Sellin, J.-F. Barthélémy, J.M. Torrenti, G. Bondonet, Delayed deformations of segmental prestressed concrete bridges: the case of the Savines Bridge, in: 1st Int. Conf. Ageing Mater. & Struct., 2014: pp. 266–273.

[51] J.-F. Barthélémy, J.-P. Sellin, J.-M. Torrenti, The effects of long-term behavior of both concrete and prestressing tendons on the delayed deflection of a prestressed structure, in: CONCREEP 10, 2015: pp. 621–630.

[52] L. Charpin, J. Niepceron, M. Corbin, B. Masson, J.P. Mathieu, J. Haelewyn, F. Hamon, M. Åhs, S. Aparicio, M. Asali, B. Capra, M. Azenha, D.E.M. Bouhjiti, K. Calonius, M. Chu, N. Herrman, X. Huang, S. Jiménez, J. Mazars, M. Mosayan, G. Nahas, J. Stepan, T. Thenint, J.M. Torrenti, Ageing and air leakage assessment of a nuclear reactor containment mock-up: VERCORS 2nd benchmark, Nucl. Eng. Des. 377 (2021). https://doi.org/10.1016/j.nucengdes.2021.111136.

[53] A. Aili, J.M. Torrenti, Modeling long-term delayed strains of prestressed concrete with real temperature and relative humidity history, J. Adv. Concr. Technol. 18 (2020) 396–408. https://doi.org/10.3151/jact.18.396.

[54] A. Aili, M. Vandamme, J.-M. Torrenti, B. Masson, J. Sanahuja, Time evolutions of non-aging viscoelastic Poisson's ratio of concrete and implications for creep of C-S-H, Cem. Concr. Res. 90 (2016) 144–161. https://doi.org/http://dx.doi.org/10.1016/j.cemconres.2016.09.014.

[55] J. Frech-Baronet, L. Sorelli, Z. Chen, A closer look at the temperature effect on basic creep of cement pastes by microindentation, Constr. Build. Mater. 258 (2020) 119455. https://doi.org/10.1016/j.conbuildmat.2020.119455.

[56] J.M. Torrenti, Basic creep of concrete-coupling between high stresses and elevated temperatures, Eur. J. Environ. Civ. Eng. 22 (2018) 1419–1428.

[57] Charpin, L., Haelewyn, J., & Mathieu, J. P. (2019, March). Identification of drying, creep and shrinkage constitutive laws for concrete at 20° C and 40° C, application to Vercors mock-up. In

Proceedings of the International Conference on Sustainable Materials, Systems and Structures (SMSS 2019), Rovinj, Croatia (pp. 20-22).